Clustering of $HClO_4$ with Brønsted (H_2SO_4, $HClO_4$, HNO_3) and Lewis acids BX_3 (X=H, F, Cl, Br, OH): A DFT study

Younes Valadbeigi[†*] and Theo Kurtén[‡*]

[†]Department of Chemistry, Faculty of Science, Imam Khomeini International University, Qazvin, Iran. Email: valadbeigi@sci.ikiu.ac.ir; Phone: +98 28 3390 1367.

[‡]Institute for Atmospheric and Earth System Research/Chemistry, University of Helsinki, PO Box 55 (A. I. Virtasen Aukio 1), FI-00014 Helsinki, Finland. Email: theo.kurten@helsinki.fi; Telephone: +358 50 526 0123.

Abstract

$HClO_4$ is an important catalyst in organic chemistry, and also acts as a reservoir or sink species in atmospheric chlorine chemistry. In this study, we computationally investigate the interactions of Brønsted (H_2SO_4, $HClO_4$, HNO_3) and Lewis acids (BH_3, BF_3, BCl_3, BBr_3, $B(OH)_3$) with $HClO_4$ using the ωB97xD method and the aug-cc-pVDZ basis set. Different isomers of clusters with up to 4 molecules (tetramer) were optimized, and the most stable structures were determined. The enthalpies, ΔH, and Gibbs free energies, ΔG, of cluster formation were calculated in the gas phase at 298 K. Atoms in molecules (AIM) calculations find B-O bond critical points only in the $(BH_3)_nHClO_4$ clusters, while formation of other clusters was based on hydrogen bonding interactions. $(H_2SO_4)HClO_4$ and $(B(OH)_3)HClO_4$, with formation enthalpies of -14.1 and -12.0 kcal mol^{-1}, were the most stable, and $(BCl_3)HClO_4$ with a formation enthalpy of -2.9 kcal mol^{-1}, was the least stable cluster among the dimers. Clustering of the Lewis and Brønsted acids with $HClO_4$ enhanced its acidity, so that clustering of four $HClO_4$ molecules and formation of $(HClO_4)_4$ increases the acidity of $HClO_4$ by about 35 kcal mol^{-1}. The most acidic dimer cluster found in the study was $(BBr_3)HClO_4$, with ΔH_{acid} of 275 kcal mol^{-1}; 26 kcal mol^{-1} stronger than that of the $HClO_4$ monomer.

Keywords: $HClO_4$; Cluster formation; Hydrogen bond; Superacidity; Lewis acid.

1. Introduction

Perchlorate (ClO_4^-) and perchloric acid ($HClO_4$) are inorganic oxidant, with numerous applications as catalysts in organic chemistry.[1] However, human exposure to these compounds leads to health risks.[2] These compounds have been found to be widespread in the soil, the atmosphere, seawater, rain and snow.[3-6] Also, there is significant evidence for the existence of perchlorate in the atmosphere and soil of Mars[7-9] and elsewhere in the Solar System.[10]

Inorganic chlorine in the stratosphere exists as Cl, ClO, HCl, $ClONO_2$, HOCl, and $HClO_4$, and about 50% of the total inorganic chlorine is in the form of $HClO_4$ (0.2 ppb).[11] Since $HClO_4$ is photochemically stable, it plays an important role as a chlorine reservoir in the stratosphere.[12] Removal of $HClO_4$ by deposition similarly represents a sink for active chlorine. It has been reported that $HClO_4$ is produced from Cl via two consecutive reactions[13,14]

$$Cl + O_3 + M \rightarrow ClO_3 + M \quad (1)$$

$$ClO_3 + OH + M \rightarrow HClO_4 + M \quad (2)$$

While reaction (1) contributes to ozone depletion, reaction (2) removes both a Cl atom and an OH radical, and thus acts as a termination step for ozone-depleting HO_x and ClO_x catalytic cycles. In addition to reaction (2), $HClO_4$ is also emitted directly to the atmosphere from anthropogenic sources such as military and industrial activities.[15] Because of strong oxidative property of perchlorate, it has been used in the production of explosives. However, most of the emitted perchlorate is used as an additive in propellants in missile engine and rockets.[16,17] A small fraction of antropogenic $HClO_4$ is thus emitted directly to the stratosphere.

Protic molecules such as $HClO_4$ can form clusters via hydrogen bonding interactions. However, to the best our knowledge, there is no systematic study on the possibility of $HClO_4$ for

participating in clustering or new–particle formation reactions. Particle formation from Brønsted acids and bases have been investigated for multiple molecules, including H_2SO_4, HNO_3, H_2O, oxalic acid, sulfonic acid derivatives, formaldehydes, amines and diamines.[18-26] Sometimes formation of these clusters has a synergic effect on the acidity enhancement, inducing spontaneous intermolecular proton transfer between the molecules in the cluster.[21] Interaction of the Brønsted acids and bases with Lewis acids such as BeX_2, BX_3, AlX_3 (X=H, F, Cl, Br), AuF_3, and SbF_5 has been also studied.[27-34] One of the famous complexes from this category is the magic acid, $HSbF_6$, with a ΔG_{acid} of 260.5 kcal mol^{-1}.[32] In contrast to the Brønsted acids, interactions with the Lewis acids mainly proceeds via charge transfer from the molecules to the empty orbitals of the Lewis acids. It has been reported that formation of the Brønsted acid/Lewis acid clusters causes a dramatic increase in the acidity, so that many of these complexes are classified as superacids, i.e. compounds more acidic than pure sulfuric acid or with a Hammet acidity function less than -12.[35] Although there is no study on the cluster formation of $HClO_4$ with Brønsted acids, the interaction of $HClO_4$ with Lewis acids AlF_3 and SbF_5 has been theoretically investigated.[33] This study showed that effect of SbF_5 on the acidity increment of $HClO_4$ is more than that of AlF_3, so that $HClO_4(SbF_5)_3$ with a ΔG_{acid} of 242.3 kcal mol^{-1},[33] is more acidic than many organic and inorganic superacids.[36-40]

Recently, we studied clusters formed from the interaction of H_2SO_4 with the Lewis acids BX_3 (X=H, F, Cl, Br, CN, OH).[41] In this work, interactions of $HClO_4$ with both Lewis and Brønsted acids, including $HClO_4$, H_2SO_4, HNO_3, BH_3, BF_3, BCl_3, BBr_3 and $B(OH)_3$, are investigated theoretically, and the stabilities of the corresponding clusters are assessed to determine whether they can be formed in either atmospheric or laboratory conditions. We also evaluate the acidity enhancement of $HClO_4$ upon clustering with these compounds.

2. Computational details

The geometries of $(HClO_4)_{1\text{-}4}$, $(H_2SO_4)_{1\text{-}3}HClO_4$, and $(BX_3)_{1\text{-}3}HClO_4$ clusters and their corresponding conjugated bases were structurally optimized using the ωB97xD functional and the aug-cc-pVDZ basis set, which includes diffuse and polarization functions for both hydrogen and heavy atoms. Recently, we used ωB97xD/aug-cc-pVDZ method for similar systems $(BX_3)_nH_2SO_4$ and confirmed its accuracy by comparison with CCSD(T)/F12 method.[41] For further validation, the geometries of $(BF_3)HClO_4$-**a**, $(BF_3)HClO_4$-**b**, and $(BF_3)ClO_4^-$ clusters were optimized at MP2/aug-cc-pVDZ level. Then, single point calculations were performed on the MP2-optimizated clusters using CCSD(T) method to obtain the relative energies. The calculated relative energies computed by ωB97xD, MP2 and CCSD(T) and geometries optimized by ωB97xD and MP2 are compared in Figure S1 (Supporting Information). Also, formation energies and acidity of $(BF_3)HClO_4$-**a,** computed by MP2 method, were included in Tables 5 & 6. Comparison of these data shows good agreement between the ωB97xD, MP2 and CCSD(T) results.

The electronic energies without thermal and zero point vibrational energy (ZPE) corrections were used to compare the stability of different isomers of each cluster. Formation enthalpies and free energies were subsequently calculated using the standard rigid rotor and harmonic oscillator approximations, a reference pressure of 1 atm, and a temperature of either 298 K or 200 K. The Gaussian 09 software was used for all calculations.[42] Quantum theory of atoms in molecules (QTAIM) was used to determine the bond critical points (BCPs) and calculate density, ρ, its Laplacian, $\nabla^2\rho$, potential, $V(r)$, and kinetic electron energy densities, $G(r)$, at BCPs. The QTAIM calculation were carried out using the AIM2000 software.[43]

3. Results and discussion

Figure 1 shows different isomers of the $(HClO_4)_n$ clusters with n=2–4, and compares their relative stabilities. Only one isomer was considered for $(HClO_4)_2$, while for $(HClO_4)_3$ and $(HClO_4)_4$ three and six isomers were optimized, respectively. In both $(HClO_4)_3$ and $(HClO_4)_4$ clusters, the isomers **a** with a cyclic structure are more stable. However, the energy difference between the isomers is small (<5 kcal mol^{-1}), likely because the isomers have the same number of hydrogen bonds.

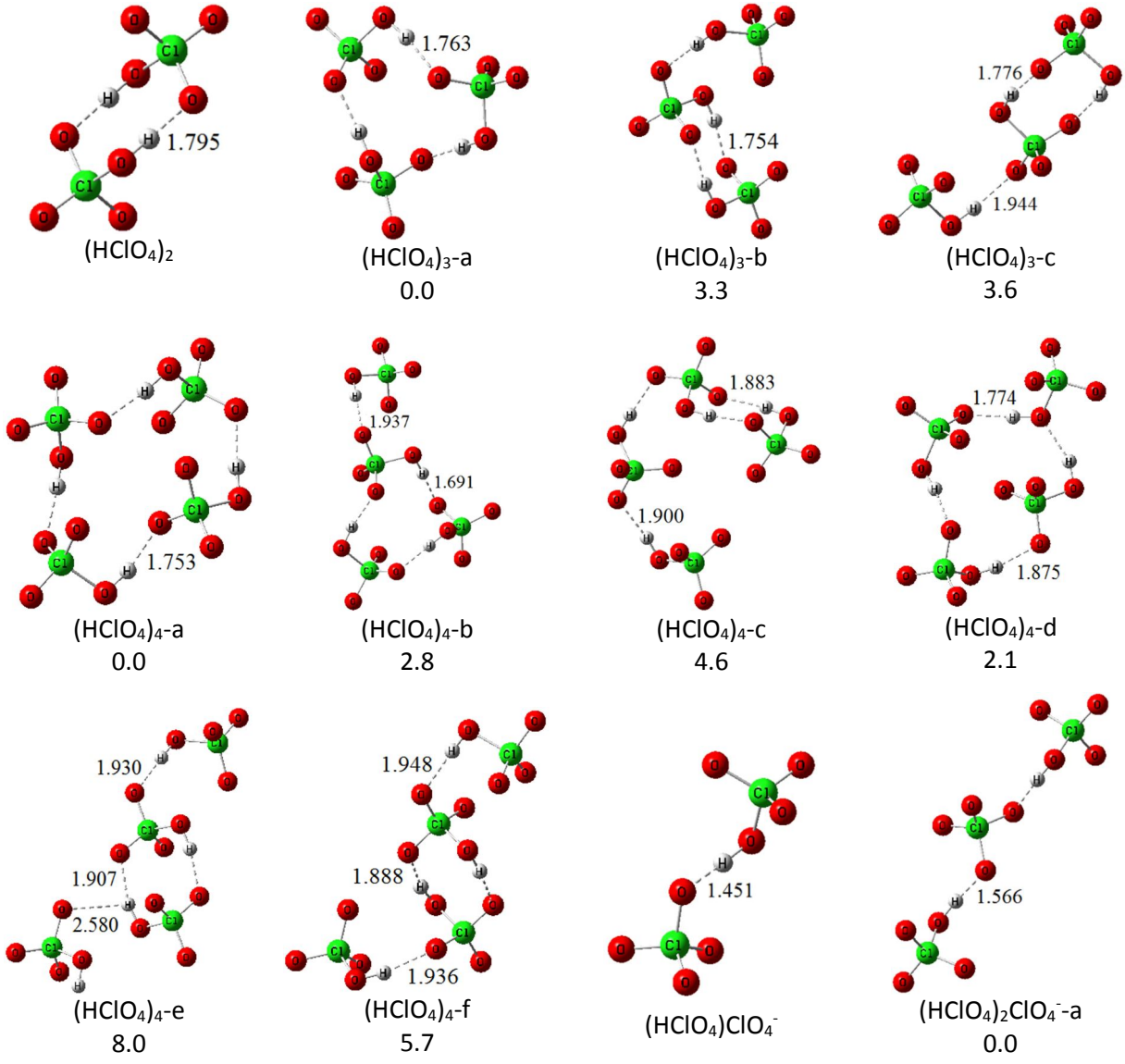

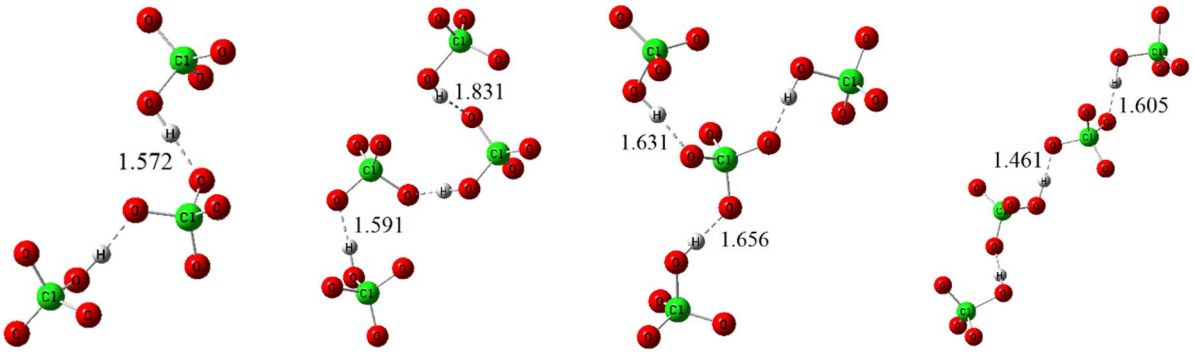

Fig. 1 Comparison of relative stabilities of different isomers of $(HClO_4)_n$ clusters, (n=2-4). The bond lengths and energies are in Å and kcal mol^{-1}, respectively. Color coding: red: oxygen, green: chlorine, grey: hydrogen.

The calculated values of the enthalpy (ΔH) and Gibbs free energy (ΔG) for formation of the $(HClO_4)_{2-4}$ clusters are summarized in Table 1. Although the formation reactions of the $(HClO_4)_{2-4}$ clusters are all exothermic, the formation ΔG values are positive because of the decrease in entropy upon clustering. Hence, the calculated equilibrium constants, K_{eq}, are all smaller than 1 (Table 1). From the K_{eq} values, the relative abundance of each $(HClO_4)_n$ cluster was obtained at 298 K for different pressure of $HClO_4$ (10^{-12}-1 atm). The relative abundances have been summarized in Table S1a (Supporting Information). To simulate the stratosphere condition, the relative abundances of the clusters were also computed at 200 K (Table S1b). Because of the small values of K_{eq}, the relative abundances of the $(HClO_4)_{2-4}$ clusters are negligible at 298 K and pressures lower than 10^{-3} atm, and $HClO_4$ exists practically solely in the monomer form. For a representative stratosphere concentration of $HClO_4$ (0.2 ppb or ~10^{-10}),[11] and at 200 K, only 10^{-6}% of the $HClO_4$ exits as dimer. The results in Tables S1a and S1b show that although $HClO_4$ clusters are not easily formed in stratosphere because of its low concentration, formation of $HClO_4$ clusters in laboratory condition is feasible. For example, at 19 °C, when $HClO_4$ is present at its saturation vapor pressure (11 Torr = 0.014 atm),[44] about 0.04% of $HClO_4$ exists as a dimer (Table S1a).

Table 1 The calculated values of enthalpy (ΔH) and Gibbs free energy (ΔG) for formation of the most stable isomers of $(HClO_4)_{2\text{-}4}$ clusters in gas phase and at 298 K

reaction	ΔH (kcal mol^{-1})	ΔG (kcal mol^{-1})	K_{eq} (1/atm)
$HClO_4 + HClO_4 \rightarrow (HClO_4)_2$	-9.5	1.9	3.57×10^{-2}
$HClO_4 + (HClO_4)_2 \rightarrow (HClO_4)_3$-a	-6.7	3.3	3.89×10^{-3}
$HClO_4 + (HClO_4)_3$-a $\rightarrow (HClO_4)_4$-a	-5.8	5.2	1.51×10^{-4}

Deprotonation of the $(HClO_4)_n$ clusters leads to formation of anionic conjugated bases, $(HClO_4)_{n-1}ClO_4^-$. The optimized structures of different isomers of $(HClO_4)_{n-1}ClO_4^-$ clusters are shown in Figure 1. The calculated enthalpies (ΔH_{acid}) and Gibbs free energies (ΔG_{acid}) for deprotonation of the $(HClO_4)_n$ clusters in the gas phase are tabulated in Table 2. The calculated ΔH_{acid} and ΔG_{acid} values for $HClO_4$ are 301.4 and 294.7 kcal mol^{-1}, respectively, indicating that $HClO_4$ is a stronger acid than H_2SO_4 with ΔH_{acid} and ΔG_{acid} values of 309.6 and 302.3 kcal mol^{-1} in the gas phase,[45] respectively. As the number of $HClO_4$ monomers increases, the acidity of the $(HClO_4)_n$ clusters increases. This may be due to stronger hydrogen bonds in the anionic conjugate bases $(HClO_4)_{n-1}ClO_4^-$, (Table S2) stabilizing the negative charge.[46,47] The ΔH_{acid} values for $(HClO_4)_2$, $(HClO_4)_3$, and $(HClO_4)_4$ are 284.7, 270-274, and 260-270 kcal mol^{-1}, respectively. Although $HClO_4$ is a stronger acid than H_2SO_4 (ΔH_{acid} = 313 kcal mol^{-1}), the acidity of $(HClO_4)_2$ is comparable to $(H_2SO_4)_2$ with ΔH_{acid} of 281-284 kcal mol^{-1}.[41,48] However, $(HClO_4)_2$ is more acidic than the heterogeneous cluster $(HNO_3)H_2SO_4$ with ΔH_{acid} of 289 kcal mol^{-1}.[41]

Table 2 The calculated values of ΔH_{acid} and ΔG_{acid} for the most stable isomers of $(HClO_4)_n$ clusters and formation the most stable conjugated bases in gas phase at 298 K

Deprotonation reaction	ΔH_{acid} (kcal mol^{-1})	ΔG_{acid} (kcal mol^{-1})
$HClO_4 \rightarrow ClO_4^- + H^+$	301.4, 298.4[a], 299.9[b]	294.7, 293.3[a]
$(HClO_4)_2 \rightarrow (HClO_4)ClO_4^- + H^+$	284.7	277.2
$(HClO_4)_3$-a $\rightarrow (HClO_4)_2ClO_4^-$-a $+ H^+$	274.1	263.9
$(HClO_4)_4$-a $\rightarrow (HClO_4)_3ClO_4^-$-b $+ H^+$	266.5	254.6

[a] calculated by B3LYP/6-311+G(d,p) from reference;[49] [b] measured experimentally.[50]

Figures 2 and 3 show the optimized structures of the $(H_2SO_4)_{1\text{-}3}HClO_4$ and $(HNO_3)_{1\text{-}3}HClO_4$ clusters and their conjugated bases, respectively. In the case of $(H_2SO_4)_{1\text{-}3}HClO_4$ clusters, the isomers with larger numbers of hydrogen bonds are usually more stable. Also, the isomers in which the $HClO_4$ is at the center of the cluster, and $HClO_4$ participates in multiple hydrogen bonds, are much higher in energy than the global minima. This may be because of weaker hydrogen bonding interactions in the $HClO_4/H_2SO_4$ and $HClO_4/HNO_3$ systems compared to those in the H_2SO_4/H_2SO_4 and HNO_3/HNO_3 systems. For example, in $(H_2SO_4)_2HClO_4$-**a**, the hydrogen bond lengths of SO–H…OCl, ClO–H…OS, and SO–H…OS, are 1.779, 1.685, and 1.640 Å, with angles of 169.9°, 173.1°, and 175.8°, respectively. Also, the calculated $\rho(r)$ values at bond critical points of these hydrogen bonds are 0.034, 0.042, and 0.046, respectively. In the case of conjugate bases, $(H_2SO_4)_2ClO_4^-$ clusters mostly have linear structures, while $(H_2SO_4)_3ClO_4^-$ clusters tend to fold and form caged structures. In all isomers, the deprotonated species is ClO_4^-, except for $(H_2SO_4)_3ClO_4^-$-**g** and $(H_2SO_4)_3ClO_4^-$-**h** in which HSO_4^- anions cluster with H_2SO_4 and $HClO_4$. However, $(H_2SO_4)_3ClO_4^-$-**g** and $(H_2SO_4)_3ClO_4^-$-**h** are considerably less stable than other isomers.

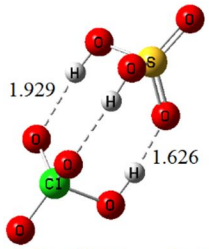

$(H_2SO_4)HClO_4$-**a** (0.0)

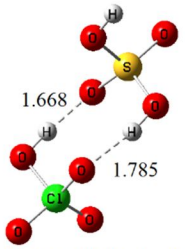

$(H_2SO_4)HClO_4$-**b** (1.1)

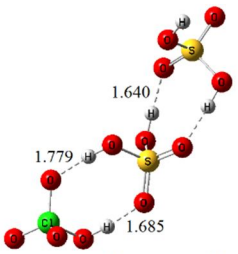

$(H_2SO_4)_2HClO_4$-**a** (0.3)

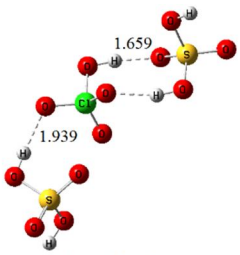

$(H_2SO_4)_2HClO_4$-**b** (12.1)

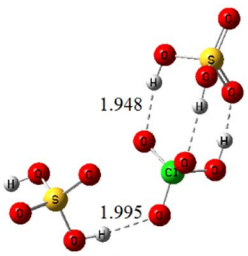

$(H_2SO_4)_2HClO_4$-**c** (11.5)

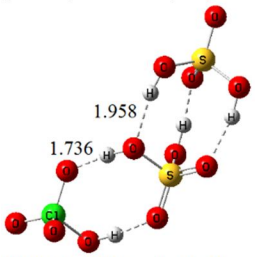

$(H_2SO_4)_2HClO_4$-**d** (0.0)

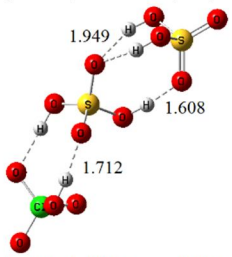

$(H_2SO_4)_2HClO_4$-**e** (2.5)

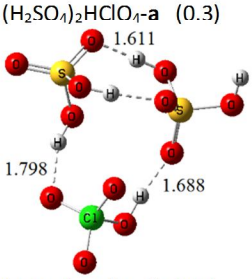

$(H_2SO_4)_2HClO_4$-**f** (2.3)

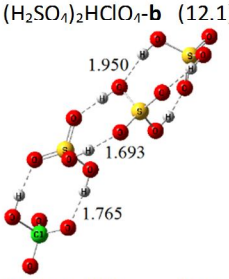

$(H_2SO_4)_3HClO_4$-**a** (0.0)

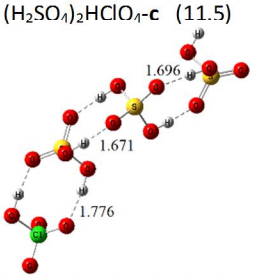

$(H_2SO4)_3HClO_4$-**b** (0.5)

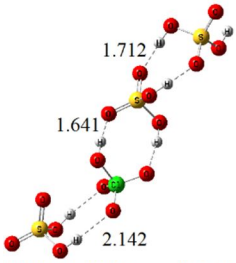

$(H_2SO_4)_3HClO_4$-**c** (12.7)

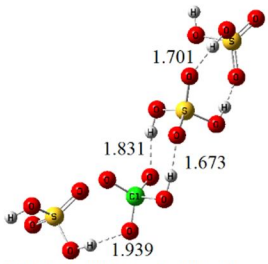

$(H_2SO_4)_3HClO_4$-**d** (12.4)

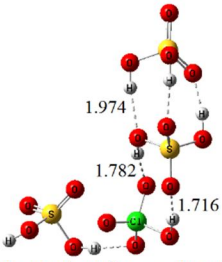

$(H_2SO_4)_3HClO_4$-**e** (12.2)

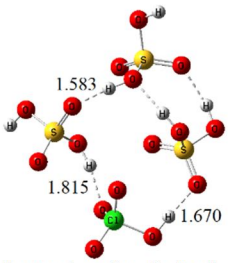

$(H_2SO_4)_3HClO_4$-**f** (9.6)

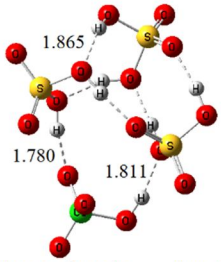

$(H_2SO_4)_3HClO_4$-**g** (11.4)

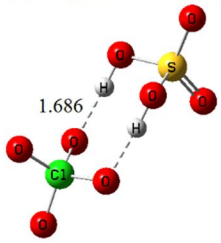

$(H_2SO_4)ClO_4^-$-**a** (0.0)

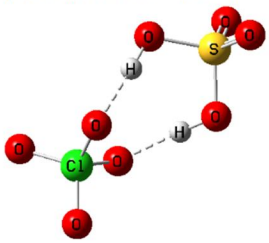

$(H_2SO_4)ClO_4^-$-**b** (1.9)

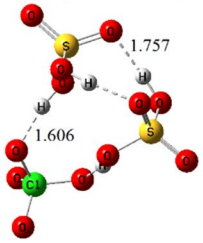

$(H_2SO_4)_2ClO_4^-$-**a** (3.7)

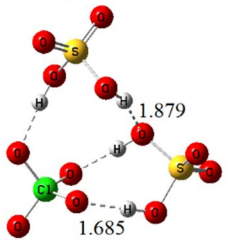

$(H_2SO4)_2ClO_4^-$-**b** (4.2)

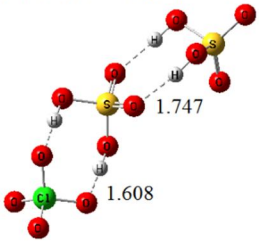

$(H_2SO_4)_2ClO_4^-$-**c** (0.0)

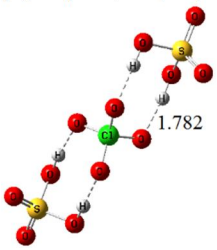

$(H_2SO_4)_2ClO_4^-$-**d** (1.6)

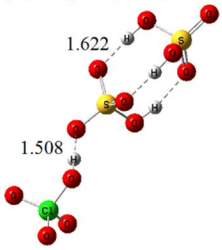

$(H_2SO_4)_2ClO_4^-$-**e** (0.8)

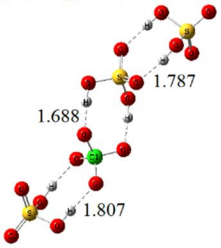

$(H_2SO_4)_3ClO_4^-$-**a** (3.6)

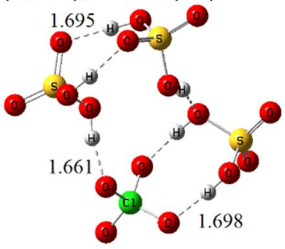

$(H_2SO_4)_3ClO_4^-$-**b** (3.7)

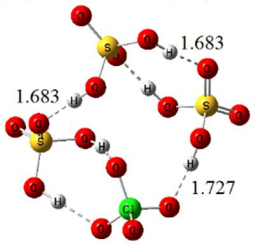

$(H_2SO_4)_3ClO_4^-$-**c** (3.4)

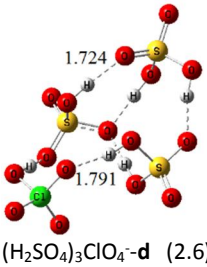

$(H_2SO_4)_3ClO_4^-$-**d** (2.6)

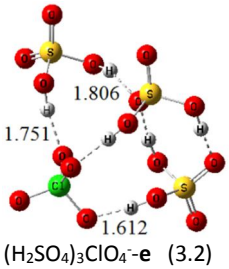

$(H_2SO_4)_3ClO_4^-$-**e** (3.2)

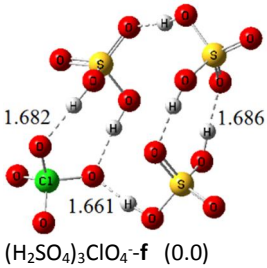

$(H_2SO_4)_3ClO_4^-$-**f** (0.0)

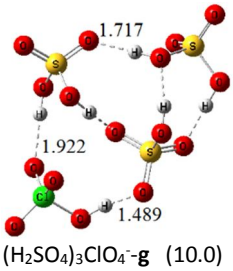

$(H_2SO_4)_3ClO_4^-$-**g** (10.0)

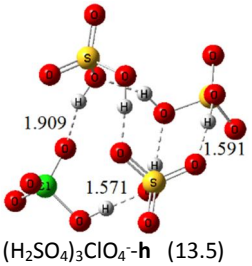

$(H_2SO_4)_3ClO_4^-$-**h** (13.5)

Fig. 2 The optimized structures of the $(H_2SO_4)_nHClO_4$ clusters and their conjugated bases, $(H_2SO_4)_3ClO_4^-$. The bond lengths and energies (numbers in the parenthesis) are in Å and kcal mol^{-1}, respectively. Color coding: red: oxygen, green: chlorine, grey: hydrogen, yellow: sulfur.

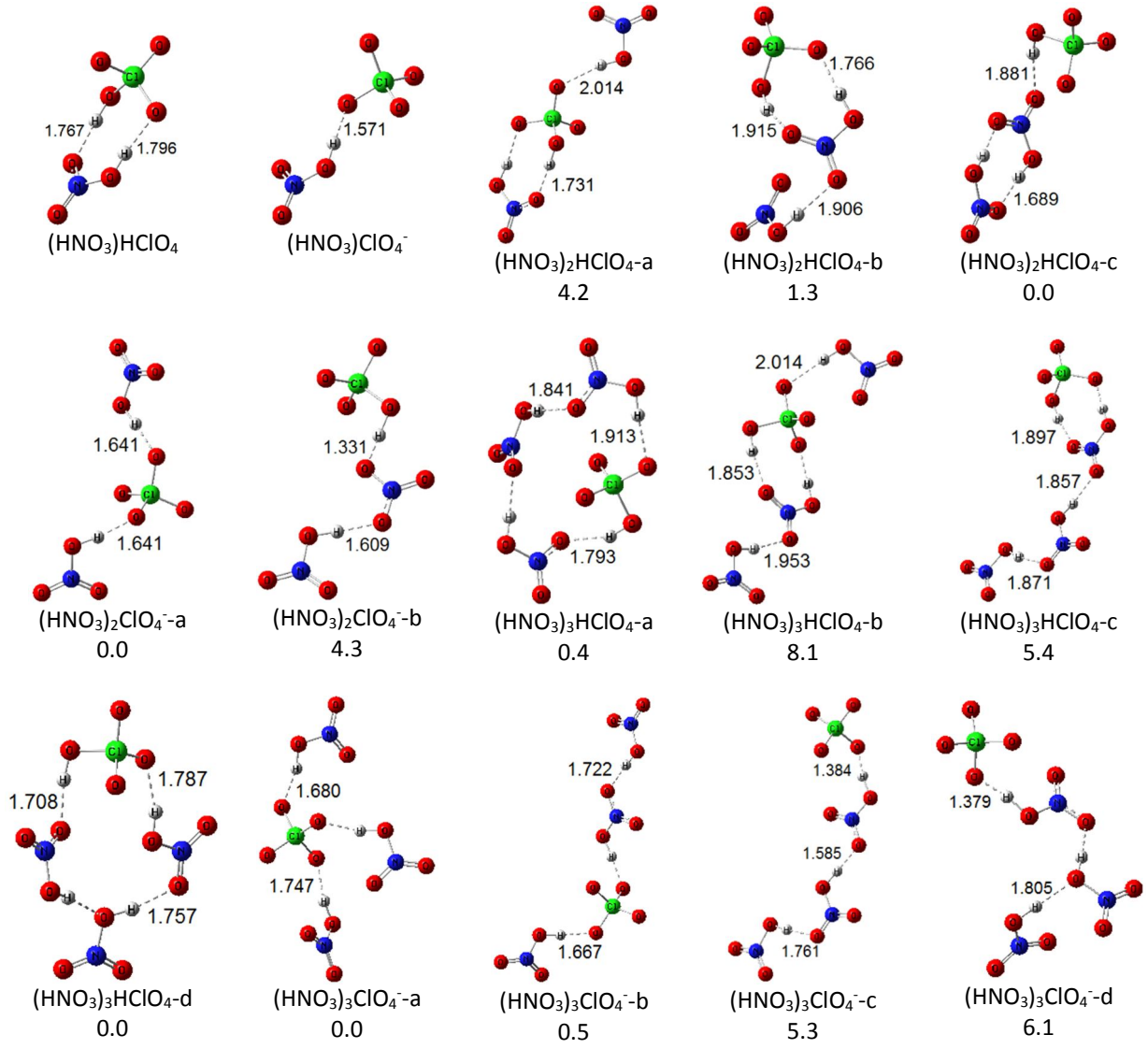

Fig. 3 The optimized structures of the $(HNO_3)_nHClO_4$ clusters and their conjugated bases, $(HNO_3)_3ClO_4^-$. The bond lengths and energies are in Å and kcal mol^{-1}, respectively. Color coding: red: oxygen, green: chlorine, grey: hydrogen, blue: nitrogen.

The calculated values of ΔH and ΔG for formation of the $(H_2SO_4)_nHClO_4$ and $(HNO_3)_nHClO_4$ clusters in gas phase are summarized in Table 3. The formation reactions of

$(H_2SO_4)_nHClO_4$ clusters are more exothermic than those of the analogous $(HNO_3)_nHClO_4$ and $(HClO_4)_{n+1}$ clusters. This may be due to the larger number of OH groups in H_2SO_4 compared to HNO_3 and $HClO_4$ allowing for the formation of more hydrogen bonds. The ΔG values show that formation of the $(H_2SO_4)_{1\text{-}3}HClO_4$ clusters is thermodynamically favorable (at a reference pressure of 1 atm), while $(HNO_3)_nHClO_4$ clusters are not formed spontaneously. While the heterogeneous $(H_2SO_4)_nHClO_4$ clusters are more stable than the corresponding homogeneous $(HClO_4)_{n+1}$ clusters, the stabilities of $(HNO_3)_nHClO_4$ and $(HClO_4)_{n+1}$ clusters are generally comparable. The general trend in stability is illustrated by the dimer interaction energies for H_2SO_4/H_2SO_4, $HClO_4/HClO_4$, HNO_3/HNO_3, HNO_3/H_2SO_4, $HNO_3/HClO_4$, $H_2SO_4/HClO_4$, which are -13.2,[51] -9.5, -8.4,[52] -10.9,[53] -9.0, and -14.1 kcal mol^{-1}, respectively. From the K_{eq} values, the relative abundances of the $(H_2SO_4)_nHClO_4$ and $(HNO_3)_nHClO_4$ clusters in H_2SO_4 and HNO_3 pressure range of 10^{-12}–1 atm and at 200 and 298 K were calculated (Tables S3 and S4). The reported saturation vapor pressure of H_2SO_4 at 296 K is ~3×10^{-8} atm.[54] Table S3a shows that in this condition and in the presence of $HClO_4$, 1.5×10^{-5}% of $HClO_4$ is as $(H_2SO_4)HClO_4$. However, it should be mentioned that self-clustering of H_2SO_4 and/or $HClO_4$ will compete with $H_2SO_4/HClO_4$ clustering. Our calculations showed that the ΔG values for formation of $(H_2SO_4)_2$, $(H_2SO_4)_nHClO_4$, and $(HClO_4)_2$ are -5.3, -1.6, and 1.9 kcal mol^{-1}, respectively. Hence, in the mixture of H_2SO_4 and $HClO_4$, the clusters $(H_2SO_4)_n$ and $(H_2SO_4)_nHClO_4$ are more abundant than $(HClO_4)_n$. The formation of $(HNO_3)_nHClO_4$ clusters is thermodynamically less favored than $(H_2SO_4)_nHClO_4$ clusters (Table 3); however, because of the higher saturation vapor pressure of HNO_3, the former clusters can more easily be generated in laboratory conditions. For example, when HNO_3 is present at its saturation vapor pressure at 298 K (0.08 atm),[55] 0.6% of $HClO_4$ exists as $(HNO_3)HClO_4$.

Table 3 The calculated values of enthalpy (ΔH) and Gibbs free energy (ΔG) for formation of the most stable isomers of $(H_2SO_4)_nHClO_4$ and $(HNO_3)_nHClO_4$ clusters in gas phase at 298 K

reaction	ΔH (kcal mol^{-1})	ΔG (kcal mol^{-1})	K_{eq} (1/atm)
$H_2SO_4 + HClO_4 \rightarrow (H_2SO_4)HClO_4$-a	-14.1	-1.6	1.53×10^{1}
$H_2SO_4 + (H_2SO_4)HClO_4$-a $\rightarrow (H_2SO_4)_2HClO_4$-d	-14.8	-3.4	2.99×10^{2}
$H_2SO_4 + (H_2SO_4)_2HClO_4$-d $\rightarrow (H_2SO_4)_3HClO_4$-a	-16.1	-5.6	1.20×10^{4}
$HNO_3 + HClO_4 \rightarrow (HNO_3)HClO_4$	-9.0	1.6	6.69×10^{-2}
$HNO_3 + (HNO_3)HClO_4 \rightarrow (HNO_3)_2HClO_4$-c	-5.3	2.7	9.55×10^{-3}
$HNO_3 + (HNO_3)_2HClO_4$-c $\rightarrow (HNO_3)_3HClO_4$-d	-8.1	0.8	2.59×10^{-1}

The calculated ΔH_{acid} and ΔG_{acid} for deprotonation of the $(H_2SO_4)_nHClO_4$ and $(HNO_3)_nHClO_4$ clusters in gas phase are summarized in Table 4. Increases in the number of H_2SO_4 and HNO_3 molecules in the clusters enhances their acidity. Although $HClO_4$ is more acidic than H_2SO_4, the $(H_2SO_4)_nHClO_4$ and $(HClO_4)_n$ clusters with the same number of molecules have comparable acidity - in many cases, the $(H_2SO_4)_nHClO_4$ clusters are actually slightly more acidic. This can be attributed to the higher stability of the $(H_2SO_4)_nClO_4^-$ clusters relative to $(HClO_4)_nClO_4^-$, which can also be seen from a comparison of the data in Tables S2 and S5 (Supporting Information). However, $(HClO_4)_n$ clusters are more acidic than the $(HNO_3)_nHClO_4$ clusters, again in accordance with the higher stability of $(HClO_4)_nClO_4^-$ clusters compared to $(HNO_3)_nClO_4^-$ (Tables S2 and S5). Interestingly, $(HNO_3)HClO_4$ and $(HNO_3)H_2SO_4$ with ΔH_{acid} values of ~289 kcal mol^{-1},[41] have the same acidity. The acidity trends in the binary clusters is $(H_2SO_4)_2 > (H_2SO_4)HClO_4 > (HClO_4)_2 > (HNO_3)HClO_4 \sim (HNO_3)H_2SO_4$. It thus seems that there is a direct relationship between the acidity of clusters and their stability, so that clusters containing H_2SO_4 are both more acidic and more stable.

Table 4 The calculated values of ΔH_{acid} and ΔG_{acid} for deprotonation of the $(H_2SO_4)_nHClO_4$ clusters in gas phase and at 298 K. Only the most stable isomers have been considered

Deprotonation reaction	ΔH_{acid} (kcal mol^{-1})	ΔG_{acid} (kcal mol^{-1})
$H_2SO_4 \rightarrow H_2SO_4^- + H^+$	313.4 (312.1)[a]	305.3 (304.5)[a]
$HNO_3 \rightarrow NO_3^- + H^+$	322.5 (324.5)[b]	315.5 (317.8)[b]
$(H_2SO_4)HClO_4$-a $\rightarrow (H_2SO_4)ClO_4^-$-a + H^+	283.7	275.8
$(H_2SO_4)_2HClO_4$-d $\rightarrow (H_2SO_4)_2ClO_4^-$-c + H^+	275.3	266.8
$(H_2SO_4)_3HClO_4$-a $\rightarrow (H_2SO_4)_3ClO_4^-$-f + H^+	270.5	265.2
$(HNO_3)HClO_4 \rightarrow (HNO_3)ClO_4^- + H^+$	289.6	280.7
$(HNO_3)_2HClO_4$-c $\rightarrow (HNO_3)_2ClO_4^-$-a + H^+	279.4	271.5
$(HNO_3)_3HClO_4$-d $\rightarrow (HNO_3)_3ClO_4^-$-a + H^+	275.9	268.4

[a]Calculated by G4 method;[56] [b]Experimental values from ref.[57]

Figure 4 shows the optimized structures of the $(BH_3)HClO_4$, $(BF_3)HClO_4$, $(BCl_3)HClO_4$, and $(BBr_3)HClO_4$ clusters. Two isomers were considered for each cluster. The "**a**" isomers containing a OH…XB (X=H, F, Cl, Br) interaction are in all cases more stable that the "**b**" isomers which lack this interaction. We expected that the boron atoms would interact with the oxygen atoms of $HClO_4$. However, the results of AIM calculations show that there is a B-O interaction only in the $(BH_3)HClO_4$ cluster, while the other clusters, including $(BF_3)HClO_4$, $(BCl_3)HClO_4$ and $(BBr_3)HClO_4$ (Table S6), lack such interactions. This can to some extent also be deduced from a comparison of the B-O bond lengths in Fig. 3. Also, BF_3, BCl_3, and BBr_3 maintain their planar geometry in the corresponding clusters, while BH_3 undergoes a planar/pyramidal conversion upon interaction with $HClO_4$. The required energy for the conversion of the planar form of BH_3 to its pyramidal structure is less than that for BF_3, BCl_3, and BBr_3.[41] Hence, BH_3 can more easily form a B-O bond with $HClO_4$. Also, because of the strong acidity of $HClO_4$, its H atom tends to form hydrogen bonds with F, Cl, and Br atoms of BX_3, and this interaction is preferred over the formation of B-O bonds. (Formation of a strong and thus short B-O bond would likely distort the H-bonding distances and angles far away from the optimum geometry, thus these two modes of interactions can be thought to compete with each other). In the case of BH_3, the interaction proceeds via B-O bond formation due to the lack of an H-bond acceptor group.

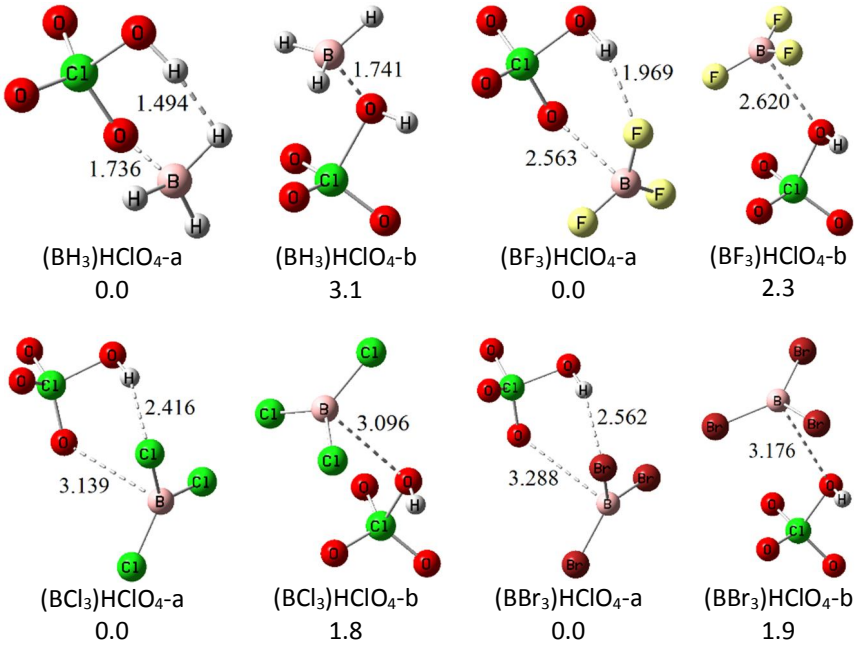

Fig. 4 The optimized structures for two isomers of the $(BH_3)HClO_4$, $(BF_3)HClO_4$, $(BCl_3)HClO_4$, and $(BBr_3)HClO_4$ clusters. The bond lengths and energies are in Å and kcal mol^{-1}, respectively. Color coding: red: oxygen, green: chlorine, grey: hydrogen, yellow: fluorine, brown: bromine, pink: boron.

The calculated values of ΔH and ΔG for formation of the $(BX_3)HClO_4$ clusters are summarized in Table 5. Comparison of the ΔH values for $BX_3/HClO_4$ interactions shows that the BH_3 has the strongest interaction with $HClO_4$, while Cl and BBr_3 show the weakest interactions. The AIM results (Table S6) show that the strong $BH_3/HClO_4$ interaction is because of a B-O bond critical point in this cluster, which is absent in other $(BX_3)HClO_4$ clusters.

In a previous study, we showed that in the $(BX_3)H_2SO_4$ clusters, the B atoms of all BX_3 molecules interact with oxygen atoms of H_2SO_4.[41] These results can be interpreted based on the fact that $HClO_4$ is a stronger acid and consequently a weaker Lewis base than H_2SO_4, and cannot easily donate its electron to an empty orbital of the B atom of BX_3.

Table 5 The ΔH and ΔG values for formation of the most stable isomers of $(BX_3)_nHClO_4$ clusters in gas phase at 298 K calculated by ωB97xD/aug-cc-pVDZ method

reaction	ΔH (kcal mol^{-1})	ΔG (kcal mol^{-1})	K_{eq} (1/atm)
$BH_3 + HClO_4 \rightarrow (BH_3)HClO_4$-a	-6.6	4.2	8.45×10^{-4}
$BF_3 + HClO_4 \rightarrow (BF_3)HClO_4$-a	-4.2, -5.5[a], -4.5[b]	4.7, 3.7[a], 4.7[b]	3.56×10^{-4}
$BCl_3 + HClO_4 \rightarrow (BCl_3)HClO_4$-a	-2.9	5.5	9.74×10^{-5}
$BBr_3 + HClO_4 \rightarrow (BBr_3)HClO_4$-a	-3.4	4.6	4.11×10^{-4}
$B(OH)_3 + HClO_4 \rightarrow (B(OH_3)HClO_4$-a	-12.0	-1.3	9.29×10^{0}
$BH_3 + (BH_3)HClO_4$-a $\rightarrow (BH_3)_2HClO_4$-c	-16.7	-5.3	7.74×10^{3}
$BF_3 + (BF_3)HClO_4$-a $\rightarrow (BF_3)_2HClO_4$-c	-2.6	5.8	5.17×10^{-5}
$BCl_3 + (BCl_3)HClO_4$-a $\rightarrow (BCl_3)_2HClO_4$-c	-2.0	5.4	1.14×10^{-4}
$BBr_3 + (BBr_3)HClO_4$-a $\rightarrow (BBr_3)_2HClO_4$-c	-4.1	4.6	4.09×10^{-4}
$B(OH)_3 + (B(OH_3)HClO_4$-a $\rightarrow (B(OH_3)_2HClO_4$-a	-10.2	-0.5	2.33×10^{0}
$BH_3 + (BH_3)_2HClO_4$-c $\rightarrow (BH_3)_3HClO_4$-c	-4.0	5.2	1.41×10^{-4}
$BF_3 + (BF_3)_2HClO_4$-c $\rightarrow (BF_3)_3HClO_4$-b	-2.1	7.0	6.75×10^{-6}
$BCl_3 + (BCl_3)_2HClO_4$-c $\rightarrow (BCl_3)_3HClO_4$-c	-2.7	7.1	6.60×10^{-6}
$BBr_3 + (BBr_3)_2HClO_4$-c $\rightarrow (BBr_3)_3HClO_4$-c	-3.8	5.5	9.41×10^{-5}
$B(OH)_3 + (B(OH_3)_2HClO_4$-a $\rightarrow (B(OH_3)_3HClO_4$-a	-10.5	0.5	4.06×10^{-1}

[a] computed at MP2/aug-cc-pVDZ level, [b] CCSD(T)/ aug-cc-pVDZ//MP2/aug-cc-pVDZ

Clusters with two and three BX_3 molecules were also considered. The optimized structures for different isomers of $(BX_3)_2HClO_4$ and $(BX_3)_3HClO_4$ are shown in Figure 5. In all clusters, the isomers with $BX_3/HClO_4$ interactions are less stable than corresponding isomers with BX_3/BX_3 interactions. Boron atoms cannot interact strongly with oxygen atoms of $HClO_4$, a weak Lewis base. Instead, B prefers to interact with X atoms of other BX_3 molecules (Table S6). Hence, the isomers **c** with BX_3/BX_3 interactions are more stable than isomers **a** with B/O interactions. Despite the energy differences between the isomers, the ΔG values in Table 5 shows that formation of all $(BX_3)_{1\text{-}3}HClO_4$ (X=H, F, Cl, Br) clusters is not thermodynamically favored, and the K_{eq} values are very small. Using the K_{eq} values, the relative abundances of the $(BX_3)_{1\text{-}3}HClO_4$ (X=H, F, Cl, Br) clusters in different pressure of BX_3 at 200 and 298 K were computed. These data have been summarized in Tables S7-S10. Comparison of the relative abundance values shows that in the pressure range of 10^{-12} to 1 atm, $HClO_4$ is present in its monomer form, as the relative concentrations of other $(BX_3)_{1\text{-}3}HClO_4$ clusters is negligible. From the relative abundances at 200 and 298 K it is concluded that formation of detectable amounts of $(BX_3)_nHClO_4$ clusters in

laboratory condition (low temperature and high concentrations of BX_3) is possible for at least those BX_3 species with high enough saturation vapor pressures.

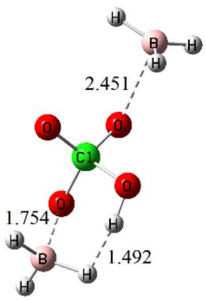

$(BH_3)_2HClO_4$-a
16.9

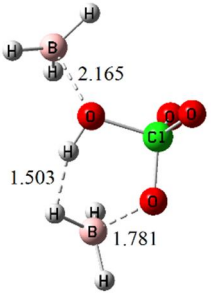

$(BH_3)_2HClO_4$-b
16.0

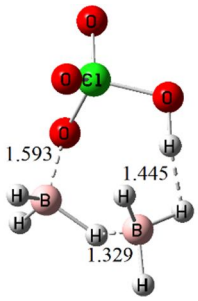

$(BH_3)_2HClO_4$-c
0.0

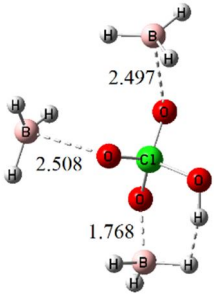

$(BH_3)_3HClO_4$-a
20.6

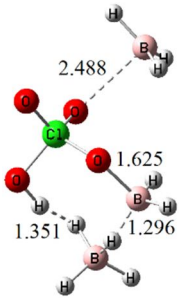

$(BH_3)_3HClO_4$-b
3.5

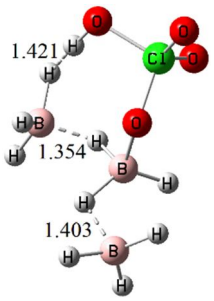

$(BH_3)_3HClO_4$-c
0.0

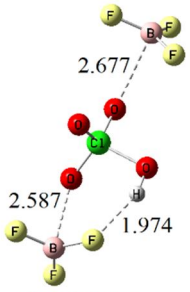

$(BF_3)_2HClO_4$-a
1.1

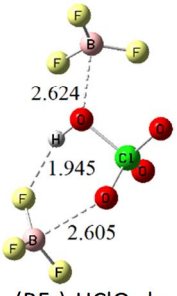

$(BF_3)_2HClO_4$-b
0.8

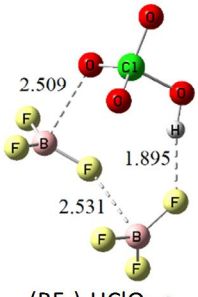

$(BF_3)_2HClO_4$-c
0.0

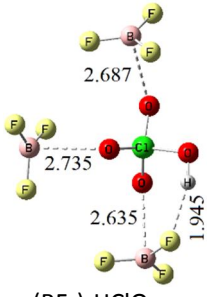

$(BF_3)_3HClO_4$-a
1.2

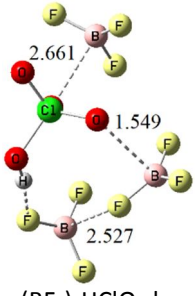

$(BF_3)_3HClO_4$-b
0.0

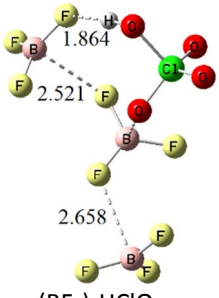

$(BF_3)_3HClO_4$-c
0.3

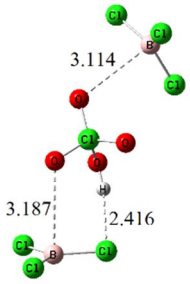

$(BCl_3)_2HClO_4$-a
1.1

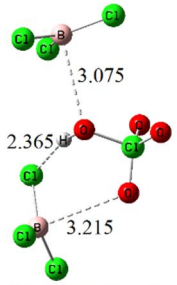

$(BCl_3)_2HClO_4$-b
0.4

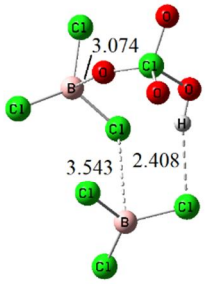

$(BCl_3)_2HClO_4$-c
0.0

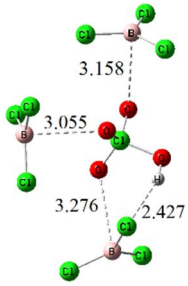

$(BCl_3)_3HClO_4$-a
1.2

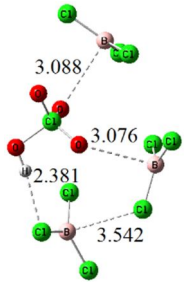

$(BCl_3)_3HClO_4$-b
0.4

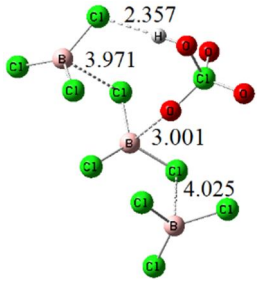

$(BCl_3)_3HClO_4$-c
0.0

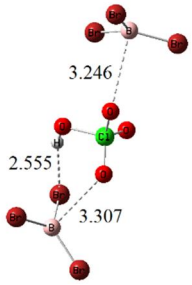

$(BBr_3)_2HClO_4$-a
2.7

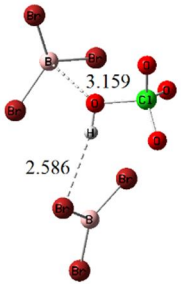

$(BBr_3)_2HClO_4$-b
0.9

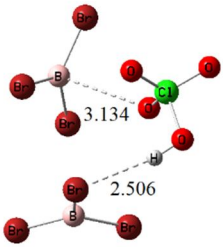

$(BBr_3)_2HClO_4$-c
0.0

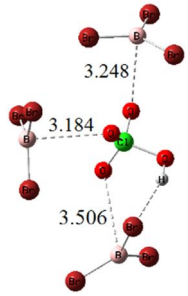

$(BBr_3)_3HClO_4$-a
2.3

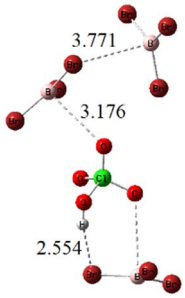

$(BBr_3)_3HClO_4$-b
3.6

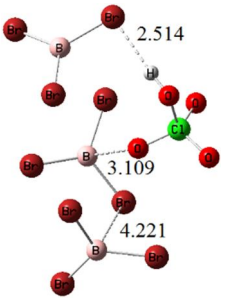

$(BBr_3)_3HClO_4$-c
0.0

Fig. 5 The optimized structures for different isomers of $(BX_3)_2HClO_4$ and $(BX_3)_3HClO_4$ cluster. The bond lengths and energies are in Å and kcal mol^{-1}, respectively. Color coding: red: oxygen, green: chlorine, grey: hydrogen, yellow: fluorine, brown: bromine, pink: boron.

Figure 6 shows the optimized structures of the conjugate bases of $(BX_3)_{1\text{-}3}ClO_4^-$ clusters. Because of the negative charge of the conjugate bases, we expect stronger B/O interactions. Comparison of the B-O bond lengths in the neutral clusters, $(BX_3)_nHClO_4$, (Fig. 5) and anionic clusters, $(BX_3)_nClO_4^-$, (Fig. 6) partially confirms our hypothesis of stronger B/O interaction in the latter. Also, AIM calculations predict B-O BCPs in all anionic $(BX_3)ClO_4^-$ clusters, while in the neutral case the BCP is present only for $(BH_3)HClO_4$. However, the existence of B/O interactions in the conjugate bases, $(BX_3)_nClO_4^-$, does not lead to considerable changes in the stability trend of the isomers of these clusters: isomers of the type $(BX_3)_nClO_4^-$**-b** with larger numbers of BX_3/BX_3 interactions are still the most stable.

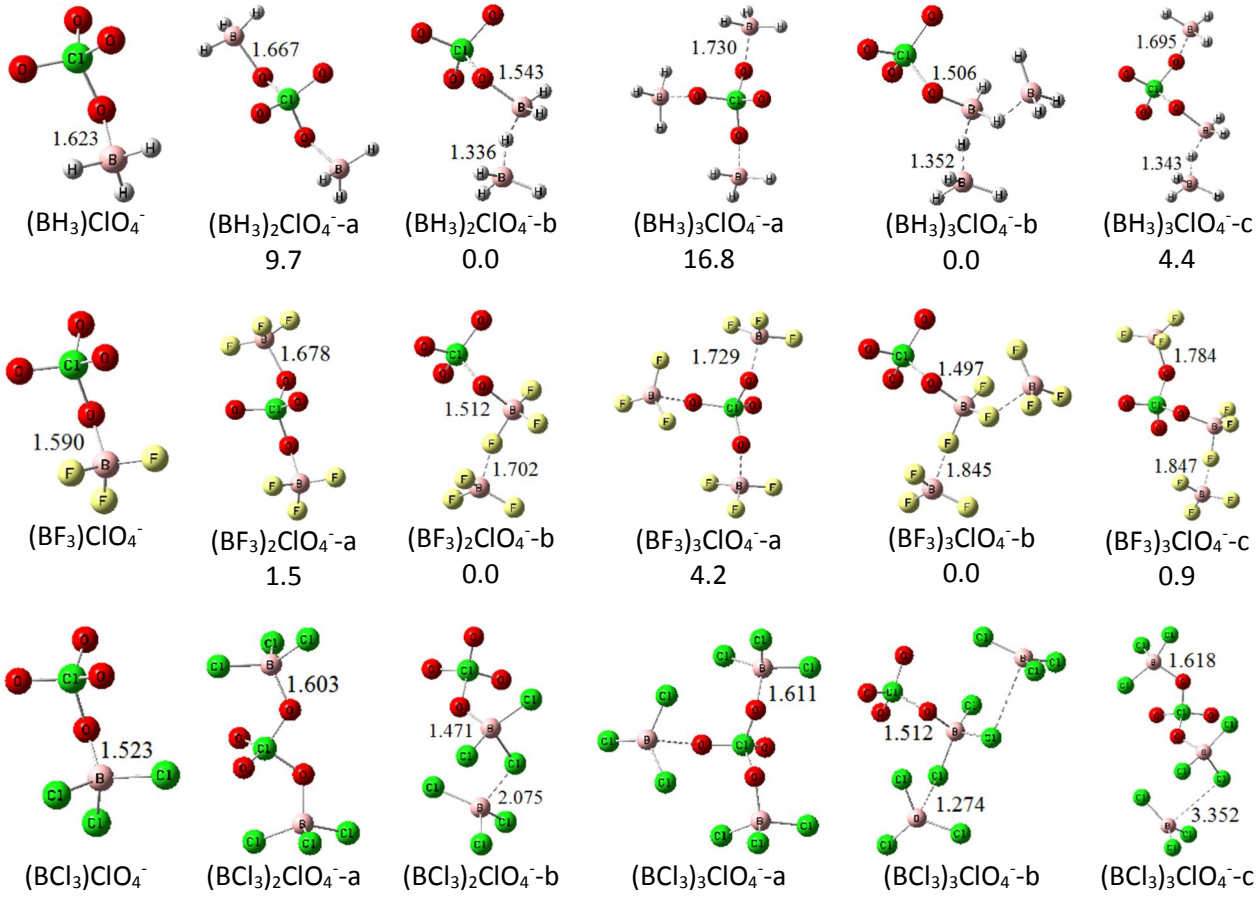

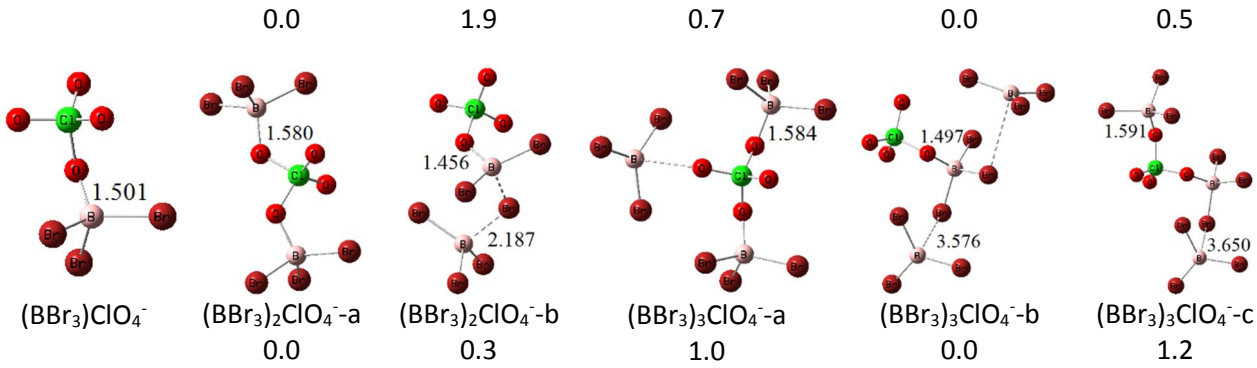

Fig. 6 Comparison of the relative stability of the isomers of $(BX_3)_2ClO_4^-$ and $(BX_3)_3ClO_4^-$ cluster. The bond lengths and energies are in Å and kcal mol^{-1}, respectively. Color coding: red: oxygen, green: chlorine, grey: hydrogen, yellow: fluorine, brown: bromine, pink: boron.

Because of B-O bond formation in the conjugate bases, $(BX_3)_nClO_4^-$, we expect that BX_3 molecules enhance the acidity of $HClO_4$. The calculated values of ΔH_{acid} and ΔG_{acid} for deprotonation of the $(BX_3)_nHClO_4$ clusters are tabulated in Table 6. For the clusters with one BX_3, the acidity increases as $(BH_3)HClO_4$ < $(BF_3)HClO_4$ < $(BCl_3)HClO_4$ < $(BBr_3)HClO_4$. This trend shows the effect of electron withdrawing groups (EWGs) on the intensifying the electron deficiency of boron, leading to stronger B/O interaction. However, the same trend does not hold for larger clusters with two and three BX_3 molecules ($(BX_3)_2HClO_4$ and $(BX_3)_3HClO_4$), as $(BH_3)_2HClO_4$ and $(BH_3)_2HClO_4$ which lack any EWGs are the strongest acids among the series. The higher acidity of $(BH_3)_nHClO_4$ clusters is due to strong H_2BH-BH_3 and ClO-BH_3 interactions in the conjugate bases. The calculated ΔH_{acid} for $(BH_3)_2HClO_4$-**b** and $(BH_3)_3HClO_4$-**b**, the most stable isomers of $(BH_3)_nHClO_4$ clusters, are 264.0 and 264.6 kcal mol^{-1}, respectively.

Table 6 The ΔH_{acid} and ΔG_{acid} values for the $(BX_3)_nHClO_4$ clusters in gas phase at 298 K calculated by ωB97xD/aug-cc-pVDZ method. Only the most stable isomers have been considered

Deprotonation reaction	ΔH_{acid} (kcal mol^{-1})	ΔG_{acid} (kcal mol^{-1})
$(BH_3)HClO_4$-a → $(BH_3)ClO_4^-$ + H^+	285.8	278.1
$(BH_3)_2HClO_4$-c → $(BH_3)_2ClO_4^-$-b+ H^+	278.7	269.8
$(BH_3)_3HClO_4$-c → $(BH_3)_3ClO_4^-$-b+ H^+	267.4	258.6
$(BF_3)HClO_4$-a → $(BF_3)ClO_4^-$ + H^+	282.2, 279.5[a], 280.6[b]	277.5, 274.6[a], 275.7[b]
$(BF_3)_2HClO_4$-c → $(BF_3)_2ClO_4^-$-b + H^+	272.6	269.3
$(BF_3)_3HClO_4$-b → $(BF_3)_3ClO_4^-$-b + H^+	267.5	263.6
$(BCl_3)HClO_4$-a → $(BCl_3)ClO_4^-$ + H^+	277.4	273.3
$(BCl_3)_2HClO_4$-c → $(BCl_3)_2ClO_4^-$-a + H^+	273.5	273.4
$(BCl_3)_3HClO_4$-c → $(BCl_3)_3ClO_4^-$-b + H^+	273.1	268.8
$(BBr_3)HClO_4$-a → $(BBr_3)ClO_4^-$ + H^+	275.0	271.3
$(BBr_3)_2HClO_4$-c → $(BBr_3)_2ClO_4^-$-a + H^+	273.2	271.9
$(BBr_3)_3HClO_4$-c → $(BBr_3)_3ClO_4^-$-b + H^+	271.7	267.7
$(B(OH)_3)HClO_4$-a → $(B(OH)_3)ClO_4^-$-b + H^+	295.3	287.5
$(B(OH)_3)_2HClO_4$-a → $(B(OH)_3)_2ClO_4^-$-b + H^+	291.6	283.9
$(B(OH)_3)_3HClO_4$-a → $(B(OH)_3)_3ClO_4^-$-a + H^+	293.4	281.9

[a] computed at MP2/aug-cc-pVDZ level, [b] CCSD(T)/ aug-cc-pVDZ//MP2/aug-cc-pVDZ

$B(OH)_3$ is a weaker Lewis acid than other BX_3 molecules, and its B atom has low tendency to interact with Lewis bases to accept electrons.[41] Because of presence of OH groups in $B(OH)_3$, it participates in cluster formation via hydrogen bonding interactions. Figure 7 shows the optimized structures of the $(B(OH)_3)_{1\text{-}3}HClO_4$ clusters and their conjugate bases. The relative stabilities of different cluster isomers have also been compared in Fig. 7. Because of existence of donor and acceptor sites in both $B(OH)_3$ and $HClO_4$, the clusters form a network of hydrogen bonds. The clusters with more hydrogen bonds are more stable. There were no intermolecular B/O interactions either in the neutral clusters $(B(OH)_3)_nHClO_4$, or in the conjugate bases, $(B(OH)_3)_2ClO_4^-$.

The calculated values of ΔH and ΔG for formation of the $(B(OH)_3)_nHClO_4$ clusters are summarized in Table 5. Unlike the $(BX_3)_nHClO_4$ (X=H, F, Cl, Br) clusters, formation of $(B(OH)_3)_nHClO_4$ is thermodynamically favored. This is because of the capability of $B(OH)_3$ to simultaneously accept and donate hydrogen bonds, and thus form more stable clusters. The calculated relative abundances of $(B(OH)_3)_{0\text{-}3}HClO_4$ clusters at different pressure of $B(OH)_3$ have summarized in Table S11. Although the relative abundances of the $(B(OH)_3)_{1\text{-}3}HClO_4$ clusters become considerable at

$B(OH)_3$ pressure higher than 10^{-5} atm and 298 K, the relative abundances of these clusters are small at the saturation vapor pressure of $B(OH)_3$, 2×10^{-9} atm.[58] Although at lower temperatures, the formation of $(B(OH)_3)_nHClO_4$ clusters is thermodynamically more favored, according to Clausius-Clapeyron equation, the vapor pressure of $B(OH)_3$ decreases as the temperature decreases, so that its saturation vapor pressure at 200 K is about 2×10^{-19} atm. Table S11b shows that in the presence of this amount of $B(OH)_3$, only 10^{-12}% of $HClO_4$ exists as $(B(OH)_3)HClO_4$.

The calculated values of ΔH_{acid} and ΔG_{acid} for deprotonation of the $(B(OH)_3)_nHClO_4$ clusters are summarized in Table 6. Although clustering of $B(OH)_3$ with $HClO_4$ enhances the acidity of $HClO_4$, the effect of $B(OH)_3$ on the acidity enhancement is smaller than that for BH_3, BF_3, BCl_3, and BBr_3. If only the most stable isomers, $(B(OH)_3)HClO_4$-**a**, $(B(OH)_3)_2HClO_4$-**a**, $(B(OH)_3)_3HClO_4$-**a** , are considered, it is found that the acidity enhancement does not depend on the number of $B(OH)_3$ groups, and is always less than 10 kcal mol^{-1}. The small acidity enhancement of $B(OH)_3$ compared to BH_3, BF_3, BCl_3, and BBr_3 is likely related to the formation of B-O bonds in the conjugate bases of the latter. While there is no B-O bond in the neutral $(BX_3)HClO_4$ clusters (X= F, Cl, Br), B-O bonds are formed upon deprotonation, leading to greater stability of the conjugate bases, and ths an enhancement of the acidity. On the other hand, the interactions in both $(B(OH)_3)_nHClO_4$ and $(B(OH)_3)_nClO_4^-$ are only hydrogen bonds. Although the hydrogen bonds in the negatively charged conjugate bases may be stronger, these stronger interactions lead to relatively smaller acidity enhancement of about 10 kcal mol^{-1}.

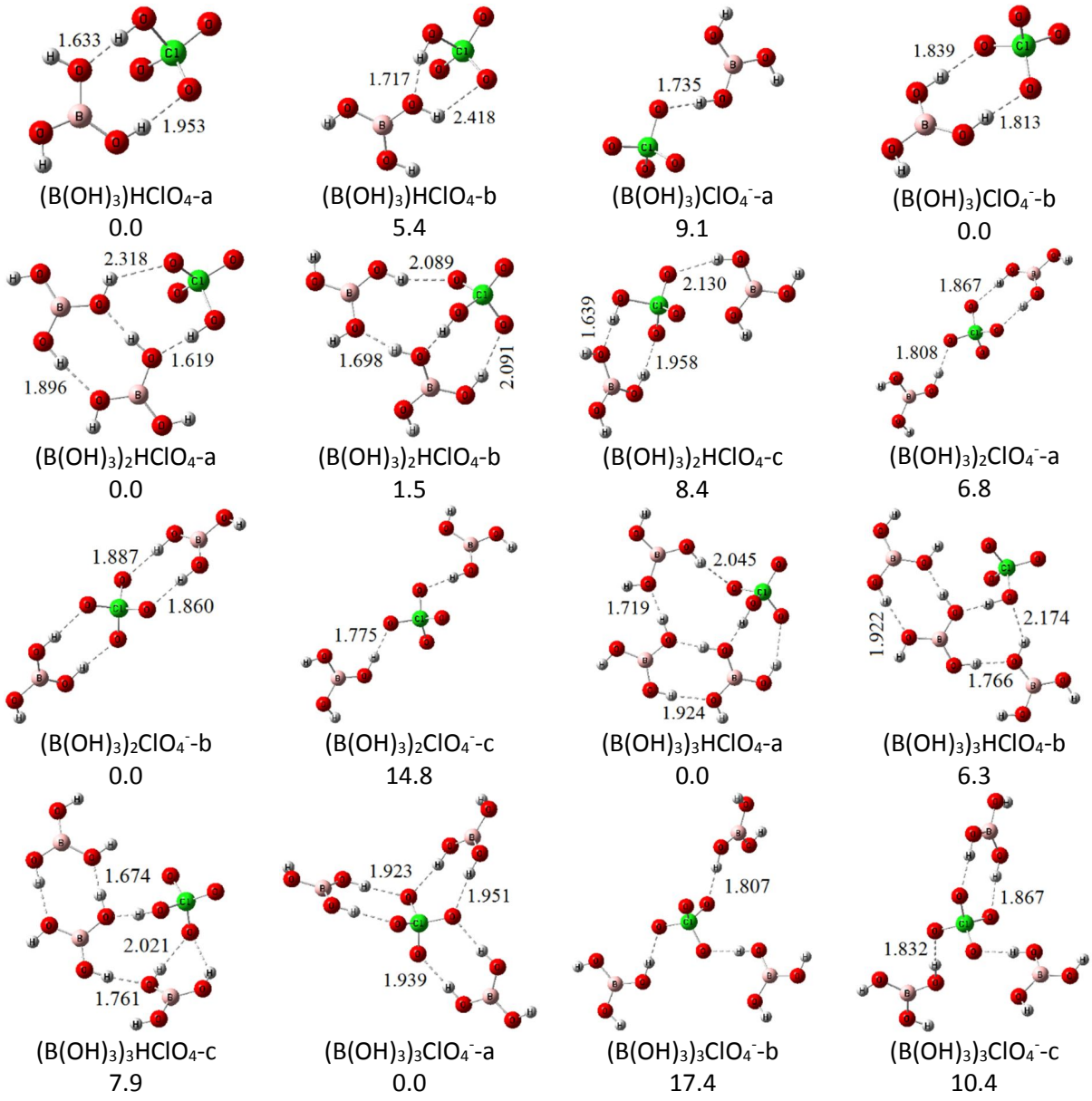

Fig. 7 Comparison of the relative stabilities of different isomers of $(B(OH)_3)_{1\text{-}3}HClO_4$ clusters and their conjugate bases, $(B(OH)_3)_{1\text{-}3}ClO_4^-$. Color coding: red: oxygen, green: chlorine, grey: hydrogen, pink: boron.

The acidity enhancement effect of the Lewis and Brønsted acids on $HClO_4$ in the binary cluster follows the order $(BBr_3)HClO_4 > (BCl_3)HClO_4 > (BF_3)HClO_4 \sim (H_2SO_4)HClO_4 \sim (HClO_4)_2 \sim (BH_3)HClO_4 > (HNO_3)HClO_4 > (B(OH)_3)HClO_4$. However, for the larger clusters this trends changes to $(HClO_4)_4 > (BH_3)_3HClO_4 \sim (BF_3)_3HClO_4 > (H_2SO_4)_3HClO_4 > (BBr_3)_3HClO_4 >$

$(BCl_3)_3HClO_4$ > $(HNO_3)_3HClO_4$ > $(B(OH)_3)_3HClO_4$. The effect of Lewis acids on the acidity enhancement of $HClO_4$ in the binary clusters is thus greater than that of the Brønsted acids. However, as the size of the clusters increases the effects of the Lewis and Brønsted acids become almost comparable. $(HClO_4)_4$ and $(BH_3)_3HClO_4$ with ΔG_{acid} values of 254.6 and 258.6 kcal mol^{-1}, respectively, are the strongest acids studied in this work. These clusters are stronger acids than $CB_{11}H_{12}H$ (ΔG_{acid}=266.5 kcal mol^{-1}),[39] $B_{12}F_1H_{11}H_2$ (ΔG_{acid}=265.2 kcal mol^{-1}),[40] $HAlF_4$ (ΔG_{acid}=269.2 kcal mol^{-1}), and HAl_2F_7 (ΔG_{acid}=261.1 kcal mol^{-1}),[39] respectively, and have comparable acidity with $HB(BF_4)_4$ (ΔG_{acid}=257.7 kcal mol^{-1}),[31] $CB_{11}F_1H_{11}H$ (ΔG_{acid}=257.2 kcal mol^{-1}), and $CB_{11}Cl_1H_{11}H$ (ΔG_{acid}=255.3 kcal mol^{-1}).[39]

4. Conclusion

Interactions of Brønsted (H_2SO_4, $HClO_4$, HNO_3) and Lewis acids (BH_3, BF_3, BCl_3, BBr_3, $B(OH)_3$) with $HClO_4$ were studied using computational methods, and clusters with up to 4 molecules (tetramers) were investigated. The Lewis and Brønsted acids interact with $HClO_4$ via hydrogen bonds, except for BH_3 in which the O atoms of $HClO_4$ interact with the B atom of BH_3. It was found that the interactions of the Brønsted acids with $HClO_4$ were stronger than the interactions of Lewis acids with $HClO_4$, except for $B(OH)_3$. Thus, clusters containing either H_2SO_4 or $B(OH)_3$ were the most stable among those investigated. The calculations showed that for a mixture of $HClO_4$ and $B(OH)_3$ at 298 K, up to 10^{-6}% of $HClO_4$ could exist as$(B(OH)_3)HClO_4$, while at 200 K (stratospheric temperature), because of the lower saturation vapor pressure of $B(OH)_3$, this amount decreases to 10^{-12}%. Clustering of both Brønsted and Lewis acids with $HClO_4$ caused acidity enhancement of $HClO_4$, with some of the clusters reaching superacidity. In the dimers, the acidity enhancement effect of the Lewis acids was greater than that of the Brønsted acids. However, in

the larger clusters, their effect on the acidity enhancement becomes equal. $B(OH)_3$ showed the smallest effect on the acidity enhancement of $HClO_4$.

Supporting Information

Comparison of ωB97xD, MP2, and CCSD(T) results (Figure S1), relative abundance of $(HClO_4)_n$ clusters (Table S1), ΔH and ΔG values for formation of $(HClO_4)_{1\text{-}3}ClO_4^-$ clusters (Table S2), relative abundance of $(H_2SO_4)_nHClO_4$ clusters (Table S3), relative abundance of $(HNO_3)_nHClO_4$ clusters (Table S4), ΔH and ΔG values for formation of $(H_2SO_4)_{1\text{-}3}ClO_4^-$ clusters (Table S5), calculated values of $\rho(r)$, $\nabla^2\rho$, $G(r)$ and $V(r)$ at the bond critical point (BCP) for interaction of $HClO_4$ and BX_3 (Table S6), structures of $(BX_3)HClO_4$ clusters (Figure S2), relative abundance of $(BH_3)_nHClO_4$ clusters (Table S7), relative abundance of $(BF_3)_nHClO_4$ clusters (Table S8), relative abundance of $(BCl_3)_nHClO_4$ clusters (Table S9), relative abundance of $(BBr_3)_nHClO_4$ clusters (Table S10), relative abundance of $(B(OH)_3)_nHClO_4$ clusters (Table S11).

Notes
The authors declare no competing financial interest.

Acknowledgments

Y.V. thanks HPC Computing Facility of IKIU, Iran, for computational resources. T. K. thanks the Academy of Finland for funding.

References

1 R. Dalpozzo, G. Bartoli, L. Sambri and P. Melchiorre, *Chem. Rev*. 2010, **110**, 3501-3551.

2 C. M. Steinmaus, *Curr. Environ. Health Rep*. 2016, **3**, 136-143.

3 D. R. Parker, *Environ. Chem*. 2009, **6**, 10-27.

4 L. G. M. B. Becking, A. D. Haldane and D. Izard, *Nature* 1958, **182**, 645-647.

5 S. Jiang, T. S. Cox, J. Cole-Dai, K. M. Peterson and G. Shi, *Geophys. Res. Lett*. 2016, **43**, 9913-9919.

6 V. I. Furdui and F. Tomassini, *Environ. Sci. Technol*. 2010, **44**, 588-592.

7 D. C. Catling, M. W. Claire, K. J. Zahnle, R. C. Quinn, B. C. Clark, M. H. Hecht and S. Kounaves, *J. Geophys. Res*. 2010, **115**, E00E11.

8 M. L. Smith, M. W. Claire, D. C. Catling and K. J. Zahnle, *Icarus* 2014, **231**, 51-64.

9 S. P. Kounaves, B. L. Carrier, G. D. O'Neil, S. T. Stroble and M. W. Claire, *Icarus* 2014, **229**, 206-213.

10 W. A. Jackson, A. F. Davila, D. W. G. Sears, J. D. Coates, C. P. McKay, M. Brundrett, N. Estrada and J. K. Bohlke, *Earth Planet. Sci. Lett*. 2015, **430**, 470-476.

11 L. Jaegle, Y. L. Yung, G. C. Toon, B. Sen and J.-F. Blavier, *Geophys. Res. Lett*. 1996, **23**, 1749-1752.

12 R. Simonaitis and J. Heicklen, *Planet. Space Sci*. 1975, **23**, 1567-1569.

13 P. K. Dasgupta, P. K. Martinelango, W. A. Jackson, T. D. Anderson, K. Tian, R. W. Tock and S. Rajagopalan, *Environ. Sci. Technol*. 2005, **39**, 1569-1575.

14 E. H. Wilson, S. A. Atreya, R. I. Kaiser and P. R. Mahaffy, *J. Geophys. Res. Planets* 2016, **121**, 1472-1487.

15 E. A. Vavricka and R. D. Morrison, *Environ. Claims J.* 2005, **17**, 193-212.

16 B. Logan, *Environ. Sci. Technol*. 2001, **35**, 482-487.

17 E. T. Urbansky, *Environ. Sci. Pollut. Res. Int*. 2002, **9**, 187-192.

18 J. Almeida, et al. *Nature* 2013, **502**, 359-363.

19 P. Ge, G. Luo, Y. Luo, W. Huang, H. Xie and J. Chen, *Chemosphere* 2018, **213**, 453-462.

20 N. Myllys, T. Olenius, T. Kurtén, H. Vehkamäki, I. Riipinen and J. Elm, *J. Phys. Chem. A,* 2017, **121**, 4812–4824.

21 J. Elm, M. Passananti, T. Kurtén and H. Vehkamäki, *J. Phys. Chem. A*, 2017, **121**, 6155–6164.

22 T. Kurtén, *Atmos. Chem. Phys.* 2019, **19**, 5033-5050.

23 K. D. Arquero, J. Xu, R. B. Gerber and B. J. Finlayson-Pitts, *Phys. Chem. Chem. Phys.* 2017, **19**, 28286-28301.

24 T. Berndt, O. Boge, F. Stratmann, J. Heintzenberg and M. Kulmala, *Science* 2005, **307**, 698-700.

25 L. Liu, H. Li, H. Zhang, J. Zhong, Y. Bai, M. Ge, Z. Li, Y. Chen and X. Zhang, *Phys. Chem. Chem. Phys*. 2018, **20**, 17406-17414.

26 P. Krishnakumar and D. K. Maity, *New J. Chem*. 2017, **41**, 7195-7202.

27 I. A. Kieffer, N. R. Treich, J. L. Fernandez and Z. M. Heiden, *Dalton Trans*. 2018, **47**, 3985-3991.

28 A. Martín-Sómer, O. Mó, M. Yáñez and J. C. Guillemin, *Dalton Trans*. 2015, **44**, 1193-1202.

29 M. Czapla and P. Skurski, *Int. J. Quantum Chem*. 2018, **118**, e25494.

30 Czapla, M.; Skurski, P. *Chem. Phys. Lett*. **2015**, *630*, 1-5.

31 A. K. Srivastava, A. Kumar and N. Misra, *J. Fluorine Chem*. 2017, **197**, 59-62.

32 M. Czapla and P. Skurski, *J. Phys. Chem. A* 2015, **119**, 12868-12875.

33 J. Brzeski, I. Anusiewicz and P. Skurski, *Theor. Chem. Acc*. 2018, **137**, 57.

34 J. Ren, C. J. Cramer and R. R. Squires, *J. Am. Chem. Soc*. 1999, **121**, 2633-2634.

35 N. F. Hall and J. B. Conant, *J. Am. Chem. Soc*. 1972, **49**, 3062-3070.

36 R. Vianello, J. F. Liebman and Z. B. Maksic, *Chem. Eur. J*. 2004, **10**, 5751−5760.

37 Y. Valadbeigi, *Int. J. Quant. Chem*. 2017, **117**, 190-196.

38 Y. Valadbeigi and R. Vianello, *Int. J. Quant. Chem*. 2018, **118**, e25754.

39 L. Lipping, I. Leito, I. Koppel and I. A. Koppel, *J. Phys. Chem. A* 2009, **113**, 12972−12978.

40 L. Lipping, I. Leito, I. Koppel, I. Krossing, D. Himmel and I. A. Koppel, *J. Phys. Chem. A* 2015, **119**, 735–743.

41 Y. Valadbeigi and T. Kurten, *Comput. Theor. Chem*. 2019, **1153**, 34-43.

42 M. J. Frisch, G. W. Trucks, H. B. Schlegel, G. E. Scuseria, M. A. Robb, J. R. Cheeseman, G. Scalmani, V. Barone, B. Mennucci, G. A. Petersson, *et al.* Gaussian 09, *Revision A.1*. Gaussian, Inc.: Wallingford, 2009.

43 F. Biegler-Konig, J. Schonbohm and D. Bayles, *J. Comp. Chem*. 2001, **22**, 545–559.

44 https://pubchem.ncbi.nlm.nih.gov/compound/Perchloric-acid#section=Odor

45 S. G. Lias, J. E. Bartmess, J. F. Liebman, J. L. Holmes, R. D. Levin and W. G. Mallard, Ion Energetics data, P. J. Linstrom, W. G. Mallard, Eds., NIST Chemistry WebBook, NIST Standard Reference Database Number 69, National Institute of Standards and Technology, Gaithersburg MD, 2010, doi:10.18434/T4D303.

46 Z. Tian, A. Fattahi, L. Lis and S. R. Kass, *J. Am. Chem. Soc*. 2009, **131**, 16984-16988.

47 H. M. Lee, A. Kumar, M. Kolaski, D. Y. Kim, E. C. Lee, S. K. Min, M. Park, Y. C. Choi and K. S. Kim, *Phys. Chem. Chem. Phys*. 2010, **12**, 6278-6287.

48 T. Kurten, T. Petaja, J. Smith, I. K. Ortega, M. Sipila, H. Junninen, M. Ehn, H. Vehkamaki, L. Mauldin, D. R. Worsnop and M. Kulmala, *Atoms. Chem. Phys*. 2011, **11**, 3007-3019.

49 I. A. Koppel, P. Burk, I. Koppel, I. Leito, T. Sonoda and M. Mishima, *J. Am. Chem. Soc*. 2000, **122**, 5114-5124.

50 M. M. Meyer and S. R. Kass, *J. Phys. Chem. A* 2010, **114**, 4086-4092.

51 J. C.; Ianni and A. R. Bandy, *J. Mol. Struct. THEOCHEM* 2000, **497**, 19-37.

52 J. R.; Hart and A. T. Takkar, *J. Mol. Struct. THEOCHEM* 2005, **714**, 217-220.

53 F. M. Balci, *Comput. Theor. Chem*. 2017, **1117**, 41-46.

54 W. Roedel, *J. Aerosol Sci*. 1979, **10**, 375-386.

55 T. E. Daubert and R. P. Danner, Physical and Thermodynamic Properties of Pure Chemicals: Data Compilation. Taylor and Francis, Washington, D. C., 1989.

56 S. Rayne and K. Forest, *J. Mol. Struc. THEOCHEM* 2010, **956**, 83-96.

57 J. A. Davidson, F. C. Fehsenfeld and C. J. Howard, *Int. J. Chem. Kinet*. 1977, **9**, 17-29.

58 R. Pankajavali, S. Anthonysamy, K. Ananthasivan and P. R. V. Rao, *J. Nucl. Mater*. 2007, **362**, 128-131.